Received: 31 July 2020 | Revised: 11 May 2021 | Accepted: 24 May 2021

DOI: 10.1002/eng2.12438

RESEARCH ARTICLE

Engineering Reports Open Access WILEY

A hybrid intelligent busbar protection strategy using hyperbolic S-transforms and extreme learning machines

Abolfazl Rahimnejad[1] | **Milad Gil**[2] | **Aliakbar Abdoos**[2] | **S. Andrew Gadsden**[1]

[1]College of Engineering and Physical Sciences, University of Guelph, Guelph, Ontario, Canada

[2]Department of Electrical and Computer Engineering, Babol Noshirvani University of Technology, Babol, Iran

Correspondence
S. Andrew Gadsden, College of Engineering and Physical Sciences, University of Guelph, Guelph, ON, Canada.
Email: gadsden@uoguelph.ca

Abstract

In power systems, busbars connect important components such as generators, transmission lines, and loads. A typical fault occurrence on the busbar may result in the isolation of faulty sections from other normally operating parts of the system resulting from differential protection operation. Although the main busbars' protection scheme is differential protection, its operation is significantly affected by magnetic saturation of the current transformer (CT), particularly during external fault occurrence or energizing power transformers. Saturation of the CT may generate a spurious differential current and is the main reason for the differential scheme malfunctioning. Previous research presented different methods to modify and improve busbars' differential protection scheme. However, there has been lack of a comprehensive study to assess the efficiency of the busbar protection scheme regarding all involved, and influencing aspects including various fault types, energizing power transformer, (high) fault resistance, fault angle (changing from 0° to 360°), and the angle of the sources. Thus, in this study, a hybrid intelligent busbar protection scheme is proposed and the effects of all these factors are investigated. The proposed strategy utilizes the hyperbolic S-transform as a signal processing technique to extract an efficient feature that is able to discriminate internal faults from other abnormal modes, that is, external faults and inrush current under CT saturation. To obtain this goal, a learning-based classification method known as extreme learning machines is used to classify the system conditions based on the selected features. The proposed protection scheme was found to have low sensitivity to CT saturation and noise and was able to accurately detect internal faults from half a cycle to one cycle of the power system depending on the fault resistance.

KEYWORDS

CT saturation, differential protection, extreme learning machine (ELM), hyperbolic S-transform, inrush current, intelligent busbar protection, support vector machine (SVM)

1 | INTRODUCTION

Busbars are the points at which power system equipment is connected. Normally, differential protection schemes are mainly utilized as the protective scheme of busbars. However, its operation can be considerably affected by the saturation of current transforms (CTs) during external faults or inrush current, which can lead to a spurious differential current so that differential protection issues an incorrect trip signal. Some researchers propose CT saturation detection techniques to modify and improve the operation of differential protection schemes in the presence of CT saturation. Authors in References 1,2 utilize a mathematical method (secondary currents' derivatives and Newton's backward difference formula) for detection and compensation of CT saturation. However, since these methods are highly noise-sensitive, it is necessary to apply a denoising filter.

Furthermore, some signal processing techniques such as wavelet transform (WT), which decompose signals into different frequency components while maintaining resolution, can be applied in busbar protection schemes.[3] In WT technique, specific filters, such as "mother" wavelets can be utilized to sequentially repeat the decomposition step for an appropriate number of times. The most important issue with WT-based techniques is that the features are extracted from the decomposed signal, specifically those from detailed levels, and are highly noise-sensitive. The number of decomposition steps that use mother wavelets requires tuning by trial and error, which can be tedious.

Some protection schemes have used artificial neural networks and fuzzy systems in order to adjust any distortion happening in the secondary current.[4,5] However, a single structure of regression tool of these intelligent methods cannot efficiently modify all distorted currents with decaying DC offset as well as different magnitudes. Moreover, due to the importance of detection time in the protection schemes, these algorithms are not an efficient tool since they require a considerable amount of time to rebuild the secondary current of CT. Authors in Reference 6 present a differential protection scheme using support vector machines to increase the accuracy of discrimination between different faulty conditions on busbars. However, the efficiency of the proposed method has not been assessed in the presence of fault resistance and inrush current.

Other than the intelligent busbar protection scheme, a couple of theoretical methods have been presented in the recently accomplished studies. Authors in Reference 7 presented a busbar protection approach based on fault components extracted from voltage and current signals. Then, it utilizes a phase-mode transformation to build aerial mode components for fault detection. A busbar protection scheme based on analysis of correlation coefficients obtained from the current of transmission lines connected to the busbar was proposed. Authors in References 8,9 also used Correlation Technique to detect busbar internal fault. Brian Johnsen et al.[10] utilized Boolean algebra and graph theory to provide a dynamic zone selection process to improve busbar protection. Researchers in References 11,12 applied initial traveling wave combined with active power differential approach to alleviate the effect of CT saturation and utilized S-transform as a signal processing technique. Authors in Reference 13 utilized WT to extract fundamental frequency components of the fault reference and virtual currents, and the angle between these two currents to describe the polarity relationship. Using this method, the authors reported an improvement in speed and reliability of the busbar protection. Euclidean distance and S-transform technique are applied in Reference 14 to analyze the similarity of the back-waves used to discriminate between internal and external faults. Researchers in Reference 15 proposed a wavelet-based method which maps restrain and operating currents into the wavelet domain and computes their energy in order to detect internal fault occurrence. The instantaneous power concept is used in Reference 16 to compute the instantaneous power of all devices connected to the busbar using the current and voltage signal.

There have been some researches utilizing hybrid methods based on signal processing techniques and intelligent classifiers to deal with various problems in the power system. Authors in Reference 17 used a combined method based on S-transform, as a signal processing technique, and extreme learning machine (ELM), as a classifier, to identify, detect, and classify power quality disturbances. Authors in Reference 18 presented a hybrid method for "islanding detection" in a distributed generation-penetrated microgrid utilizing S-transform and ELM. Moreover, ELM as a classifier is utilized in Reference 19 to locate the fault in high-voltage direct current transmission lines. In Reference 19, WT and S-transform are used to extract proper features from current signals. A combined method based on mathematical morphology and ELM was proposed in Reference 20 to detect and classify different fault events in a microgrid. In order to increase the detection and classification accuracy, a denoising filter was applied to the signal. Authors in Reference 21 implemented a novel high-impedance fault protection technique based on wavelet packet transform and ELM; this strategy could also be used as a protection scheme for the transmission and distribution lines.

Although in some proposed methods, the detection accuracy seems adequate, the detection speeds are relatively low which is of paramount importance in protection schemes. Moreover, in most of the literature, the effects of highly noise-corrupted signal, high impedance of fault, and various types of faults (including single line to ground (SLG), double line to ground (DLG), line to line (LL), three-phase (3Ph), and three phases to ground (3PhG)) on their proposed methods have not been fully assessed. In addition, to the best of the authors' knowledge, none of the previous studies investigated the effect of inrush current on the detection accuracy of the intelligent protection scheme. Consequently, in this paper, we propose a hybrid intelligent busbar protection scheme based on hyperbolic S-transform (HST), as a signal processor, and ELM, as a classifier. The extracted feature from the differential current using HST is added to the same quantities used in the percentage differential protection of busbars. To realize this goal, amplitudes of differential and restraint currents are used to distinguish internal faults from external faults and inrush current as well. In the proposed method, the HST signal processing tool is utilized to evaluate the differential current in both frequency and time domains to extract an appropriate feature used for the classification purpose. Adding this new feature to the previously used quantities in the busbar protection scheme creates distinguishing regions in the feature space which can be categorized utilizing a proper classifier.

The main contributions and advantages of the proposed busbar protection scheme in this paper are: (1) high accuracy in discriminating internal faults from other abnormal modes, that is, external faults and inrush current, through the use of several features simultaneously; (2) high-speed fault detection in 10 ms up to 20 ms, where the latter is related to some cases with high impedance faults; (3) insensitivity to noise; (4) maintaining accuracy in the presence of current transformer (CT) saturation; (5) no requirement to change the architecture of the protective infrastructures of the power system that is useful for easier implementation (6) considering the effect of impedance of faults (up to 800 Ω), the angle of fault occurrence (complete range between 0° and 360°), and the sources' angle on detection accuracy of the proposed method (7) working efficiently under the values of fault resistance for which the algorithm has not been trained.

The rest of the paper is organized as follows. General busbar protection strategies are summarized in Section 2, and the proposed hybrid intelligent busbar protection strategy is discussed in Section 3. In Section 4, simulation results are presented and discussed, followed by concluding remarks in Section 5.

2 | BUSBAR PROTECTION

Busbars are considered as nodes of the power systems to connect different components. When an incorrect busbar trip signal is issued because of protection scheme maloperations (commonly caused by CT saturation in the presence of external fault or inrush current), the probability of system instability increases.

Differential protection is extensively utilized as the main protection scheme for different components like busbars in power systems. One of the differential protection strategies which is considered as a fast busbar protection approach is high-impedance protection.[22] This configuration uses a high impedance in the differential operation path, which is typically 1000 Ω up to 2000 Ω. During an internal fault occurrence, the differential current passing through this high impedance leads to a considerable voltage drop which would be detectable by an overvoltage relay. This approach is sensitive and fast; however, it may experience a malfunctioning (issuing a wrong trip signal) under CT saturation caused by the external fault or inrush current.

The most common commercial strategy used in busbar differential protection is a percentage-differential type. Its configuration is shown as follows in Figure 1.[22]

As can be observed in Figure 1, the addition of certain restraint coils to an operation coil (overcurrent relay) creates the differential protection configuration. Different types of characteristics are provided to the designers. The trip zone of this protection scheme is formulated and characterized based on the following equations:

$$\begin{aligned} &I_{OP} > g(I_{RES}); \quad Trip := Operation \\ &I_{OP} = I_{DIF} = |i_1 + i_2 + \ldots + i_n| \\ &I_{RES} = f(|i_1| + |i_2| + \ldots + |i_n|) \end{aligned} \tag{1}$$

where $i_1, i_2, \ldots, i_n$ are corresponding to currents flowing through feeders 1 to n. Note that these currents can pass in both directions based on fault types. Based on Equation (1), if the differential current I_{DIF} is higher than the

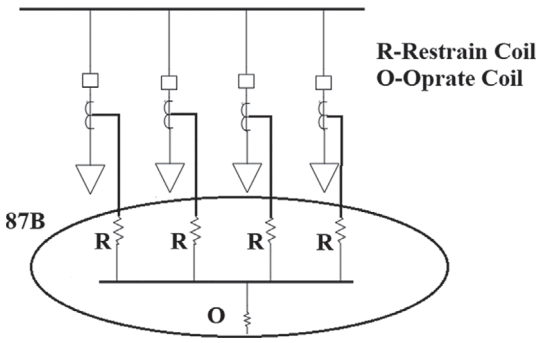

FIGURE 1 Percentage differential protection configuration[22]

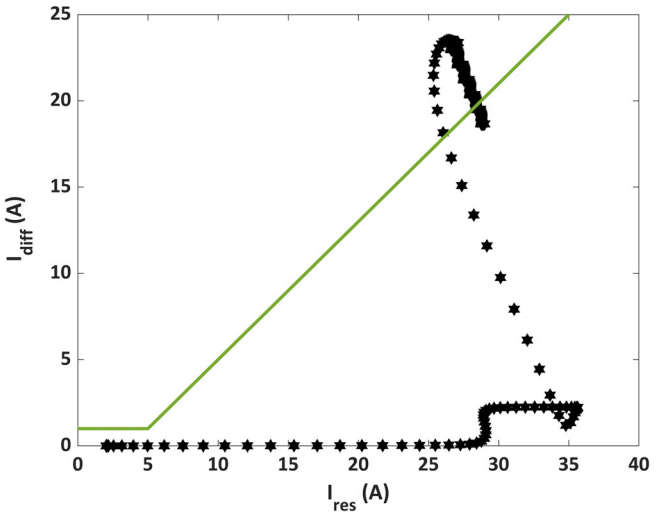

FIGURE 2 Differential protection scheme maloperation under CT saturation applied to the strategy proposed by Siemens. Note that the black dots represent the operating current (of the differential relay). The region above the green line represents a "trip zone," and the region below the green line represents a "safe zone"

value of a predefined function of restraining current I_{RES}, the trip signal is issued to the circuit breaker (CB) to isolate the faulty busbar from other normally operating parts of the grid.[22] It is noteworthy that various types of characteristics can be designed by changing the functions $g(I_{RES})$. Also, the restraint current is constructed using the $f(.)$ function that can be selected from various types of function, proposed by the standards, based on the system configuration.

Percentage protection techniques are employed to avoid maloperation of relays during external faults. However, this protection method nevertheless cannot entirely segregate between internal and external faults. Figure 2 illustrates the malfunctioning, caused by CT saturation, of percentage differential protection schemes presented by Siemens.[23] As can be observed, CT saturation (after I_{RES} reaches 35 A) yields a reduction in restrain current (I_{RES}) and an increment in differential current (I_{DIF}); as a result, the operating point goes to the trip region during external faults, and consequently, the wrong trip signal is issued to the CB to detach the busbar from other parts of the system leading to further power system issues.

In this regard, the most important issues that endanger the busbar protection scheme is the maloperation of the relay due to saturation of the CT caused by faults outside the busbar protection zone and consequently, the issuance of the wrong trip signal for the faults occurring outside of its protective zone.[22] Also, energizing the power transformer can lead to malfunctioning of the relay and busbar protection. Therefore, in this paper, an intelligent busbar protection scheme is presented for distinguishing internal faults from the external faults and inrush currents, which also takes into consideration comprehensive fault modes (Fault types, fault resistance, fault angels).

3 | PROPOSED HYBRID INTELLIGENT BUSBAR PROTECTION STRATEGY

In this paper, a hybrid busbar protection scheme is implemented based on HST to extract an appropriate feature to discriminate among different power system conditions including internal faults, external faults, and inrush currents. Based on the selected features ELM is used to classify two classes of busbar protective conditions whether it experiences internal fault or not. To achieve this purpose HST is applied as a signal processing tool and ELM is employed for classification purposes, classifying between an internal fault and other power system conditions including inrush current and external fault. The flowchart of the proposed scheme is depicted in Figure 3.

3.1 | Hyperbolic S-transform

The S-transform is an invertible time–frequency distribution which is a combination of elements of short-time Fourier transform and WT. This technique utilizes a Gaussian window whose width and height scales inversely and linearly, respectively, with frequency. The S-transform representation of $h(t)$ is as follows[24]:

$$S(\tau,f)=\int_{-\infty}^{+\infty}h(t)\{w(\tau-t)exp(-2\pi ift)\}dt \tag{2}$$

where f is the frequency, $\tau$is a parameter with which the Gaussian window's position on the t-axis can be controlled, and w is Gaussian window for each time which is defined as follows[24,25]:

$$w(t)=\frac{|f|}{\sqrt{2\pi}}exp\left(\frac{-t^2f^2}{2}\right) \tag{3}$$

The S-transform provides a multi-resolution analysis containing the absolute phases along with the related frequency contents. However, the Gaussian window, utilized in this S-transform, does not have any parameters to adjust its width in both the time and frequency domains. Authors in References 25 generalize an S-transform which has control over the Gaussian window function. This method uses an extra symmetrical window for the higher frequency ranges where the window is narrowed down, and the time resolution is larger. An additional asymmetrical window might be deployed at the lower frequency ranges, where the window is wider and the resolution in the frequency domain does not provide critical information. This extra window may be used to eliminate the event occurring on the less critical frequency resolution

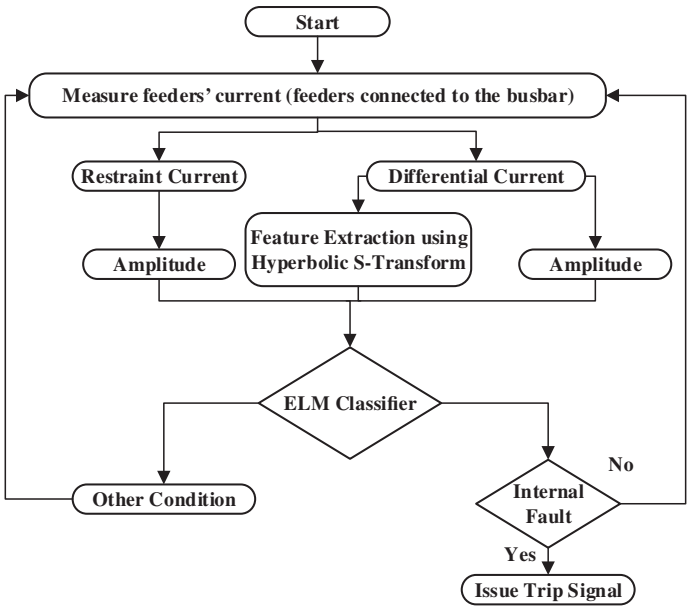

FIGURE 3 Flowchart of the proposed busbar protection strategy

within the S-transform window. This concept was utilized by the authors in Reference 25 to present a pseudo-Gaussian window called a hyperbolic window w_{Hyp}, which is defined as follows[25]:

$$w_{Hyp} = \frac{2|f|}{\sqrt{2\pi}(\gamma^F_{Hyp} + \gamma^B_{Hyp})} exp\left\{ \frac{-f^2[X(\tau - t, \{\gamma^F_{Hyp}, \lambda^B_{Hyp}, \lambda^2_{Hyp}\})]^2}{2} \right\} \tag{4}$$

where we have the following:

$$X(\tau - t, \{\gamma^F_{Hyp}, \gamma^B_{Hyp}, \lambda^2_{Hyp}\}) = \frac{\gamma^F_{Hyp} + \gamma^B_{Hyp}}{2\gamma^F_{Hyp}\gamma^B_{Hyp}}(\tau - t - \zeta) + \frac{\gamma^F_{Hyp} - \gamma^B_{Hyp}}{2\gamma^F_{Hyp}\gamma^B_{Hyp}}\sqrt{(\tau - t - \zeta)^2 + \lambda^2_{Hyp}} \tag{5}$$

where X is a hyperbolic function in $(\tau - t)$ which is dependent on parameters including backward-taper γ^B_{Hyp}, forward-taper γ^F_{Hyp} $(0 < \gamma^F_{Hyp} < \gamma^B_{Hyp})$, and a positive curvature λ_{Hyp} in time units. In order to ensure that the peak of w_{Hyp} occurs at $(\tau - t) = 0$, we can define ζ as follows:

$$\zeta = \sqrt{\frac{(\gamma^B_{HY} - \gamma^F_{HY})^2\lambda^2_{HY}}{4\gamma^B_{HY}\gamma^F_{HY}}} \tag{6}$$

It is worth mentioning that HST, with the exploitation of the above-mentioned improvement (compared to the original S-transform), reduces energy levels of (S-contours) during the external faults and inrush current occurrence. This makes the proposed index more efficient to be used to discriminate internal faults from external faults and inrush currents.

3.2 | ELM for busbar protection

ELM method was initially presented for single-layer feed-forward neural networks (SLFNs) and then modified and improved for the generalized SLFNs.[26] Researchers widely utilize feed-forward neural networks in many fields due to their capability of feature mapping in complicated nonlinear problems. It provides an efficient model for problems that need to handle a large class of natural and artificial events, which is computationally challenging for other conventional parametric methods.[26]

ELM provides some advantages which make it a powerful choice for classification problem. Firstly, it can be utilized for multiclass classifications (or regression) without having access to diverse variants needed for different problems.[27] Secondly, based on ELM theory, it can be implemented with widespread sorts of feature mapping[27] and tuning is not needed for the hidden layer.[27] In addition, the hidden nodes of ELM are chosen randomly and the output weights of SLFN are determined analytically.[26] These features make ELM a fast and robust algorithm applicable to the protection schemes whose quick and precise operation is of paramount importance.

The output function of ELM for the generalized SLFNs is denoted as follows[26]:

$$f(x) = h(x)\beta = \sum_{i=1}^{L} \beta_i h_i(x) \tag{7}$$

where β is the vector of the weights between the L nodes of the hidden layers and the output, and $h(x)$ is the feature mapping function which maps data from the input space (d dimensions) to the hidden layer space (L dimensions). Equation (8) defines the decision function for the problem of binary classification[26]:

$$f(x) = sign(h(x)\beta) \tag{8}$$

It is worth noting that our investigated problem, that is, discriminating between internal fault and other conditions (external fault or inrush current), is a binary classification problem. In comparison with the conventional classification algorithms, the objective function of the ELM model is the minimization of the training errors and norm of output weights.

This way of defining objective function improves its generalization performance, based on Bartlett's theory.[26] Equation (9) provides the objective function of the ELM model[26]:

$$Minimize : ||H\beta - T||^2 \; and \; ||\beta|| \tag{9}$$

where the output matrix of the hidden layer is denoted as H:

$$H = \begin{bmatrix} h(x_1) \\ \vdots \\ h(x_N) \end{bmatrix} = \begin{bmatrix} h_1(x_1) & \dots & h_L(x_1) \\ \vdots & \vdots & \vdots \\ h_1(x_N) & \vdots & h_L(x_N) \end{bmatrix} \tag{10}$$

As can be observed from (9), if we try to minimize the norm of the output weights $\|\beta\|$, it would be equal to the maximization of the marginal distance of two different classes ($2/\|\beta\|$) in the ELM feature space.[26]

4 | SIMULATION RESULTS AND DISCUSSION

The test system is shown in Figure 4. It was firstly modeled in PSCAD software and included various parameters that were used to generate the simulation results. Data were extracted from the CTs used for the protection of 'Busbar 1' shown in Figure 4.[6] In the simulation, the turn-ratio of the CTs is set at 2000:5. Different fault types (see Table 1), the time of fault occurrence, that is, different fault occurrence angle changing from 0 to 360° by a step of 7.2°, the phase angle of the sources, and several fault resistances (including high values up to 800 Ω) are considered in the simulation. For the phase angle of the sources, two values of 0° and 10° have been applied. It should be mentioned that various fault types, investigated in this study (including SLG, DLG, LL, 3Ph, and 3PhG), have been applied to the test system (Figure 4) in PSCAD software and their associated differential currents are extracted. Further information on the number of each

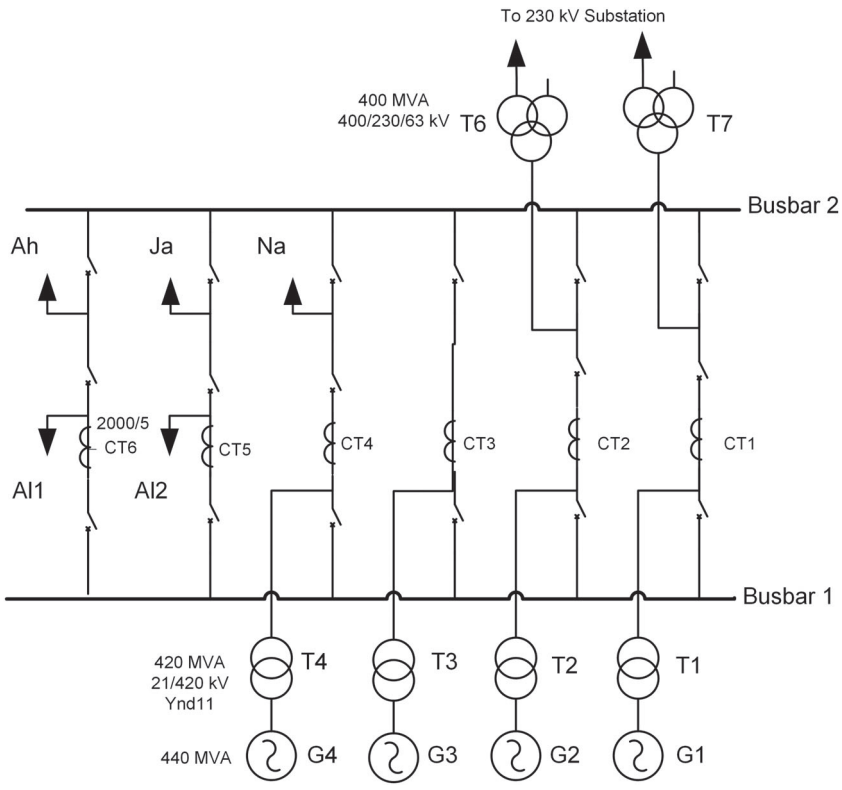

FIGURE 4 Test system used; breaker and half-busbar arrangement[6]

TABLE 1 Number of each fault type and inrush current considered in the simulation

Modes	SLG	DLG	LL	3Ph	3PhG	Inrush current
External fault	70	70	70	70	70	-
Internal fault (Solid)	70	70	70	70	70	-
Internal fault (50 Ω)	70	70	70	70	70	-
Energizing power transformer	-	-	-	-	-	100

fault type and inrush current considered in the simulation is presented in Table 1. CT parameters and Core specification according to Jiles–Atheton model are also presented in Tables A1 and A2, respectively, in Appendix A. Simulation was carried out on a computer with Intel Core i5 6300U 2.50 GHz processor with 8 GB RAM.

4.1 | Signal processing using HST

As mentioned, in this study, the HST method is applied to differential currents under various distinct abnormal conditions (internal fault, external fault, and inrush current) in MATLAB. Appropriate features from differential current signals are extracted and used to determine if an abnormal condition can be regarded as an internal fault or not (Binary classification). Figure 5(A)–(C) show the S-matrix contour of differential current caused by a typical internal fault, external fault, and inrush current, respectively. During external faults and inrush current occurrence with CT saturation, some harmonic orders, such as second-order along with high-frequency components are generated. Note that, high-frequency components caused by external fault will last for a longer time compared to inrush current under CT saturation (see Figure 5(B),(C)). However, during the occurrence of internal faults, the fundamental harmonic order, that is, 50 Hz frequency of power system, is the main component that exists in the S-matrix contour of differential current (see Figure 5(A)), with negligible existence of higher-order harmonic components. As observed, the magnitude of S-contour during internal fault is considerably higher than that of the other conditions (external fault or inrush current) when CT is under saturation, which provides an appropriate feature to make internal faults detectable.

4.2 | The generated index

Investigation of these S-matrix contours which are connected to different conditions determines that there is a substantial difference between energy levels of the first and second S-matrix contours of differential current (during the internal fault, external fault, and inrush current occurrences). Moreover, comparing the spectrum of the differential current for different conditions, an obvious difference exists between the ratio of the fundamental component to the second and third ones. Based upon the results, the multiplication of these features, such as the S-matrix contours' energy levels and harmonic order ratios, provides a sufficient margin for discriminating internal faults from other modes. This creates an appropriate feature to separate internal faults from external faults and inrush current (as illustrated by Figure 6). Consequently, the generated index is defined as follows[6]:

$$Index = |E_{l1} - E_{l2}|R_{12}R_{13} \tag{11}$$

where E_{l1} and E_{l2} are energies of the first and the second level of S-matrix contours, respectively. Furthermore, R_{12} and R_{13} are the ratios of the fundamental component of the differential current spectrum to its second and third orders, respectively.

4.3 | Detection strategy

The objective of our proposed detection strategy is to categorize the busbar protective condition in two different classes whether it experiences an internal fault or other conditions, that is, external fault and inrush current. To realize this

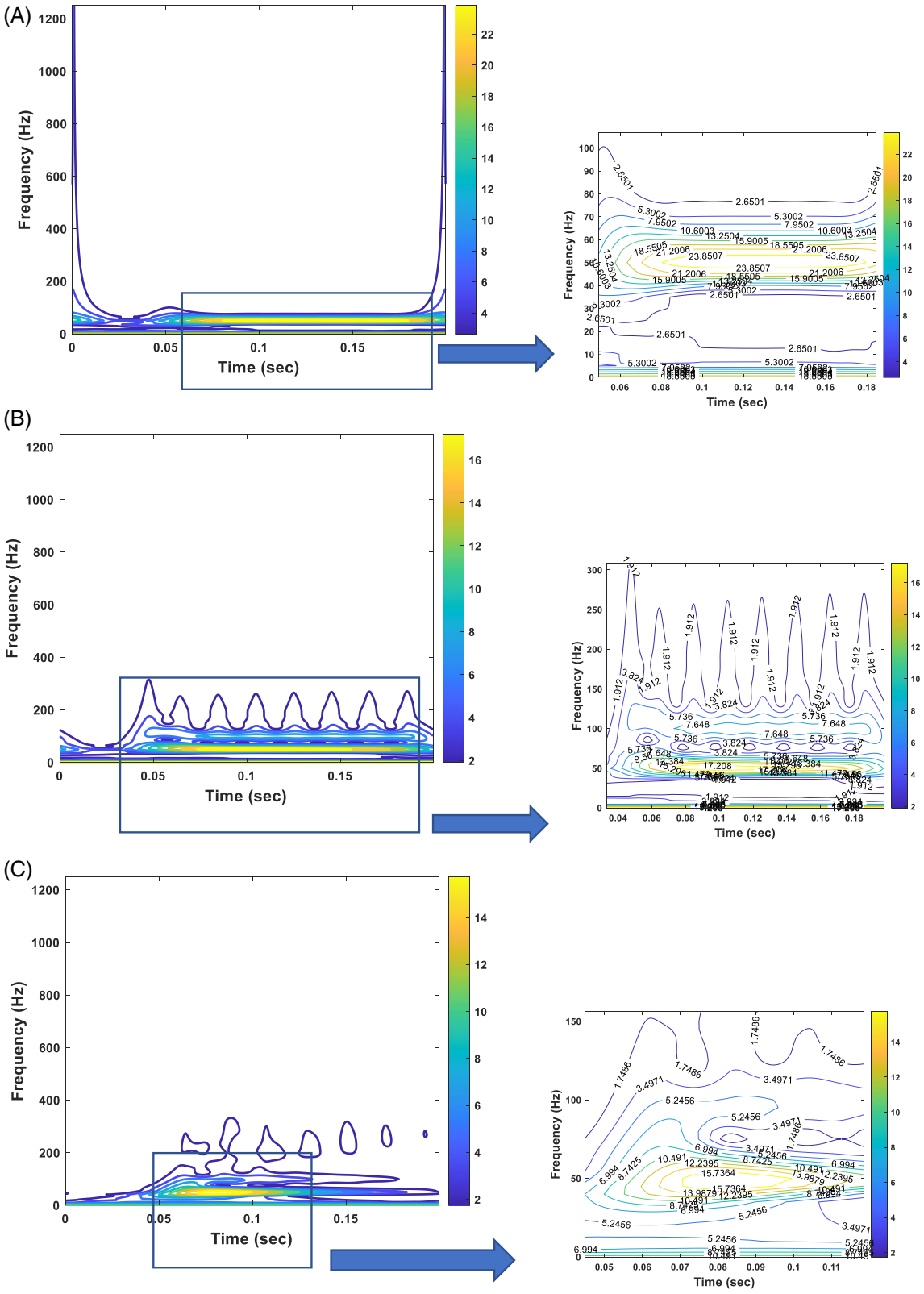

FIGURE 5 (A) S-matrix contour of differential currents computed by HST during an internal fault. (B) S-matrix contour of differential currents computed by HST during an external fault under CT saturation. (C) S-matrix contour of differential currents computed by HST during an Inrush current with CT saturation

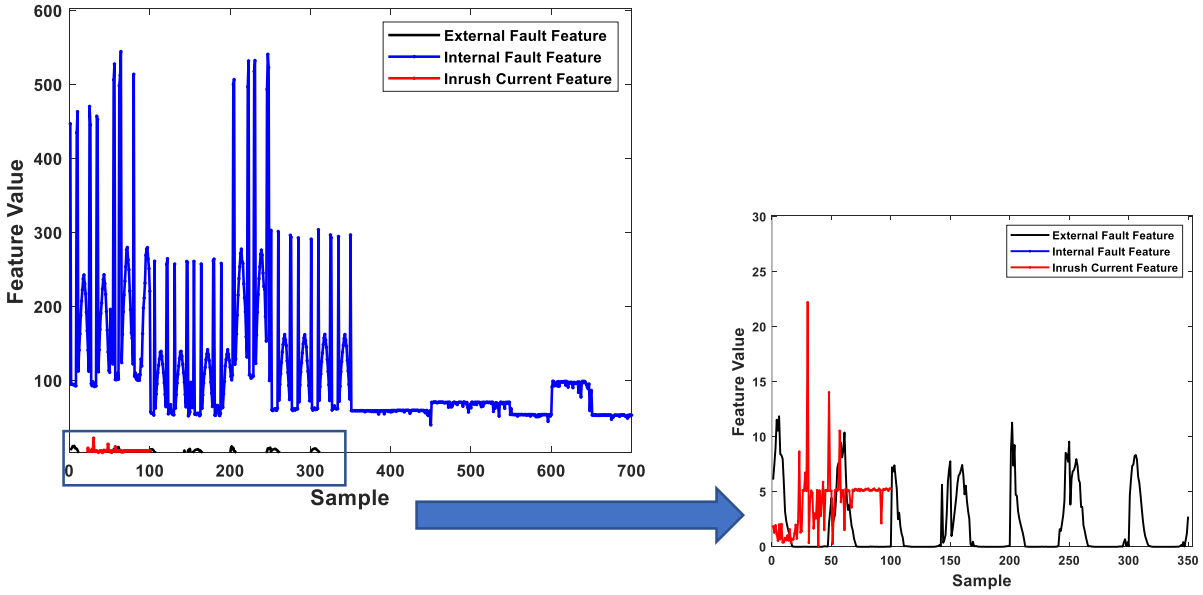

FIGURE 6 The generated feature for internal, external faults, and Inrush current (1150 total samples)

goal, the values of the amplitude of restraint and differential currents utilized in the percentage differential protection along with the extracted feature using HST analysis are used to segregate internal faults from other abnormal conditions. To implement the learning stage of the classification algorithm (ELM), 350 cases of external faults under CT saturation, 700 cases of internal faults (350 solid [without fault resistance] cases and 350 cases with 50 Ω fault resistance), 100 cases of inrush current (all extracted from the simulation) are used to train and test the ELM model in the MATLAB environment. Note that data (differential current, restrain current, and the proposed index) extracted from all cases are shuffled and then, 85% of them are randomly selected for training and the remaining (15%) are used for testing. The number of hidden neurons of the ELM classifier is set to 500, and Hardlim function is chosen as the activation function of ELM.

Moreover, it is important to note that the features are normalized between 0 and 1 to efficiently teach the ELM strategy, as well as to mitigate the undesired influence of the wide-range variation of the extracted features. Thus, the ELM model output returns a binary classification, with 1 for the internal faults and 0 for other abnormal conditions. The 3D presentation of the extracted feature for different abnormal conditions is shown in Figure 7(A). As illustrated, the added extracted feature to the conventional differential scheme has created distinguishable regions in the feature space, which allows efficient segregation of internal faults using an appropriate classifier such as the ELM strategy. Note that the detection of the internal fault from the other abnormal conditions under CT saturation would be challenging for the conventional differential scheme (see Figure 7(B)). The training and average test time of the proposed algorithm are 19.5 and 0.9 ms, respectively.

4.4 | Evaluation of the generated index under noisy condition

To improve the simulation results, all cases of faulty operation modes as well as inrush currents (1050 cases) are utilized to validate the trained algorithm under noisy conditions (with signal to noise ratio of 20 dB). Note that the waveforms of differential current (for all abnormal cases) are extracted from the simulation of the test system in PSCAD software and then, these signals are corrupted by Gaussian noise in MATLAB software. ELM passed all of the investigated cases with no misclassification of internal faults (without any false positive and false negative detection).

According to Figure 8(A)–(C), the proposed busbar protection strategy has a high speed of operation and is able to detect the internal faults in one-half cycle up to a whole cycle (detection time increases with the increment of the fault resistance up to a whole cycle). According to Figure 8(B),(C), the proposed protection scheme accurately detects internal faults even with insignificant amplitudes of differential current related to the relatively higher values of fault resistance

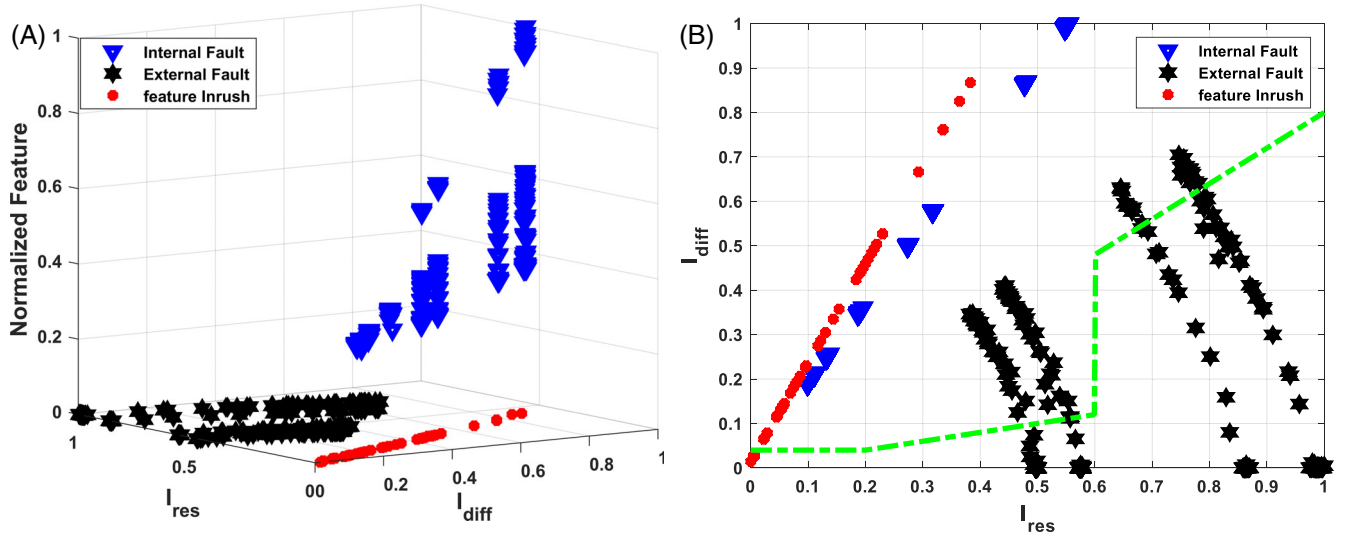

FIGURE 7 (A) 3D representation of the extracted features for different abnormal modes. (B) Illustration of the implemented cases based on differential ($I_{\text{diff}} - I_{\text{res}}$) characteristics of the conventional scheme

(up to 800 Ω). Moreover, as observed in Figure 8(C), the proposed scheme can efficiently detect internal fault with 800 Ω fault resistance while it has been trained just for either the solid (without fault resistance) cases or 50 Ω fault resistance. The same performance of the proposed algorithm has been observed for the values of fault resistances higher than 50 Ω up to 800 Ω. These aforementioned advantages may be considered as a noticeable achievement of the present study. As observed from Figure 8(A)–(C), the fault of three demonstrated cases (chosen among all the investigated cases) occurs at different angles.

It is also worth mentioning that although the relay sees a considerable differential current for both inrush current and external fault cases (shown in Figure 8(D),(E), respectively), it does not issue a trip signal in the proposed protection scheme. Note that the inrush current leads to a higher differential current in magnitude than external fault but lasting for a lower time. Moreover, the differential currents caused by energizing power transformer and external fault under CT saturation (non-sinusoidal waveform) are both significantly higher than one caused by the internal fault.

The obtained results also confirm that the generated index still works as a suitable feature to distinguish the internal faults from other modes, even while the current is affected by a considerable amount of noise (as per Figure 8). The efficient operation of the proposed intelligent protection scheme increases the stability of the power system and improves the power system reliability.

4.5 | Summary of a comparative study

To evaluate the efficiency of the proposed protection scheme, a couple of recently published articles in the area of busbar protection have been considered and compared with the present study (see Table 2). As mentioned earlier, the accuracy of the proposed method (hybrid protection scheme based on HST and ELM) is found to be 100%. Note that even for the higher magnitude of noise with the existence of relatively high fault resistance and changing angle of fault occurrence, our proposed scheme can still accurately (with 100% accuracy) discriminate the internal faults from both external fault and inrush current.

Note that since the busbar protection scheme proposed in the current study is based on a training-and-testing procedure utilizing a well-defined index, its accuracy can be numerically calculated. On the other hand, the methods presented in the articles[9,11,16] are theoretical approaches, whose accuracy is not reported (let us assume the authors claim that the accuracy of a theoretical method is 100%). However, for real-world conditions such as the existence of inrush current, higher levels of noise, higher fault resistances, and/or a wider range of fault angles, the accuracy of these theoretical methods is not guaranteed to be maintained.

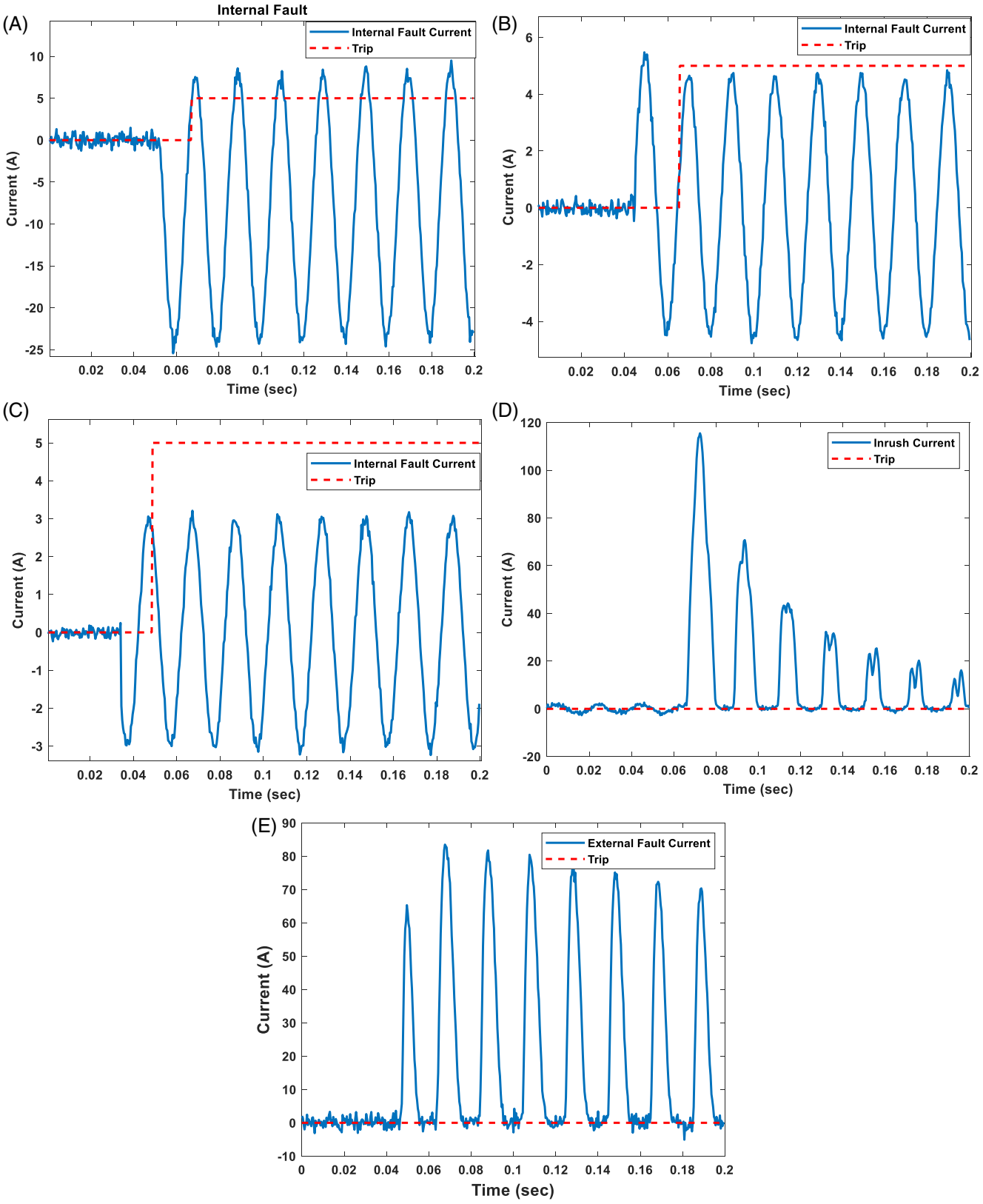

FIGURE 8 (A) Differential current and trip signal with 20 dB SNR and an internal fault (solid case). (B) Differential current and trip signal with 20 dB SNR and an internal fault with fault resistance 50 Ω. (C) Differential current and trip signal with 20 dB SNR and an internal fault with fault resistance 800 Ω. (D) Differential current and trip signal with 20 dB SNR and an inrush current. (E) Differential current and trip signal with 20 dB SNR and an external fault with CT saturation

TABLE 2 Comparative study

	SNR	Inrush current	Fault resistance (Ω)	Fault angle (°)	Accuracy
Current study	20 dB	Yes	0–800	0–360	100%
6	20 dB	No	-	0–180	100%
9	-[a]	No	0-100	-	-
11	30–70 dB	No	0–800	5–100	-
16	50 dB	No	0–300	0–180	-

[a]Dash (–) means "not reported."

5 | CONCLUSIONS

In this paper, we present a hybrid intelligent method for protecting busbars against various types of abnormal modes. A signal processing technique, that is, HST, was implemented to extract an appropriate feature based on analyzing the differential current in both the time and frequency domains. This was completed in order to efficiently segregate internal faults from other abnormal modes (external faults and inrush current). The new extracted features along with common features of percentage differential protection scheme, such as the magnitude of differential and restraint currents, were utilized for training a classification tool. An ELM was applied to classify between two conditions whether an internal fault in the busbar protection zone occurred or not. According to the results, the proposed protection scheme was found to have low sensitivity to CT saturation and noise, and was able to accurately detect internal faults in one-half up to a whole cycle of the power system. The ability to rapidly and accurately detect faults happening in the protective busbar zone is extremely important for any busbar protection schemes and helps improve the overall reliability and stability of power systems. Categorizing the various internal fault types, and locating the busbar zone at which fault occurred using an appropriate classifier may be considered as future works.

CONFLICT OF INTEREST

The authors declare no potential conflict of interest.

AUTHOR CONTRIBUTIONS

Abolfazl Rahimnejad: Conceptualization; formal analysis; investigation; methodology. **Milad Gil:** Conceptualization; formal analysis; investigation; methodology. **Ali Akbar Abdoos:** Investigation; methodology; project administration. **Stephen Andrew Gadsden:** Project administration; resources; writing-review & editing.

PEER REVIEW

The peer review history for this article is available at https://publons.com/publon/10.1002/eng2.12438.

DATA AVAILABILITY STATEMENT

The data that support the findings of this study are available from the corresponding author upon reasonable request.

ORCID

Aliakbar Abdoos https://orcid.org/0000-0003-0973-9349
S. Andrew Gadsden https://orcid.org/0000-0003-3749-0878

REFERENCES

1. Hooshyar A, Sanaye-Pasand M, Davarpanah M. Development of a new derivative-based algorithm to detect current transformer saturation. *IET Gener Transm Distrib*. 2012;6(3):207. https://doi.org/10.1049/iet-gtd.2011.0476
2. Chothani NG, Bhalja BR. New algorithm for current transformer saturation detection and compensation based on derivatives of secondary currents and Newton's backward difference formulae. *IET Gener Transm Distrib*. 2014;8(5):841-850. https://doi.org/10.1049/iet-gtd.2013.0324
3. Eissa MM. New differential busbar characteristic based on high frequencies extracted from faulted signal during current transformer saturation. *IET Gener Transm Distrib*. 2014;8(4):619-628. https://doi.org/10.1049/iet-gtd.2013.0038

4. Khorashadi-Zadeh H, Sanaye-Pasand M. Correction of saturated current transformers secondary current using ANNs. *IEEE Trans Power Deliv*. 2006;21(1):73-79. https://doi.org/10.1109/TPWRD.2005.858799
5. Hong YY, Wei DW. Compensation of distorted secondary current caused by saturation and remanence in a current transformer. *IEEE Trans Power Deliv*. 2010;25(1):47-54. https://doi.org/10.1109/TPWRD.2009.2034820
6. Gil M, Abdoos AA. Intelligent busbar protection scheme based on combination of support vector machine and S-transform. *IET Gener Transm Distrib*. 2017;11(8):2056-2064. https://doi.org/10.1049/iet-gtd.2016.1686
7. Zou G, Song S, Zhang S, Li Y, Gao H. A novel Busbar protection based on the average product of fault components. *Energies*. 2018;11(5):1139. https://doi.org/10.3390/en11051139
8. Ibrahim MR, Abd-Elatif AS, Mohammed SM. A novel Busbar protection based on correlation technique. Paper presented at: Proceedings of the 2019 21st International Middle East Power Systems Conference, MEPCON 2019, Cairo, Egypt; December 2019:491-495. https://doi.org/10.1109/MEPCON47431.2019.9007912.
9. Jena S, Bhalja BR, Samantaray SR. A fault zone identification scheme for Busbar using correlation coefficients analysis. Paper presented at: Proceedings of the IEEE Power and Energy Society General Meeting, Atlanta, GA; August 2019. https://doi.org/10.1109/PESGM40551.2019.8973764.
10. Bainy RG, Silva KM, Lotfifard S, Guzman A, Johnson BK. Dynamic zone selection for Busbar protection based on graph theory and Boolean algebra. *IEEE Trans Power Deliv*. 2019;35(4):1-1. https://doi.org/10.1109/TPWRD.2019.2953594
11. Wu H, Dong X, Wang Q. A new principle for initial traveling wave active power differential Busbar protection. *IEEE Access*. 2019;7:70495-70512. https://doi.org/10.1109/ACCESS.2019.2917044
12. Wu H, Dong X, Ye R. A new algorithm for busbar protection based on the comparison of initial traveling wave power. *IEEJ Trans Electr Electron Eng*. 2018;14(4):tee.22835. https://doi.org/10.1002/tee.22835
13. Wu H, Dong X, Wang Q. New principle of busbar protection based on a fundamental frequency polarity comparison. *PLoS One*. 2019;14(3):e0213308. https://doi.org/10.1371/journal.pone.0213308
14. Dong X, Peng Q, Wu H, Chang Z, Yue Y, Zeng Y. New principle for busbar protection based on the Euclidean distance algorithm. *PLoS One*. 2019;14(7):e0219320. https://doi.org/10.1371/journal.pone.0219320
15. Silva KM, Escudero AMP, Lopes FV, Costa FB. A wavelet-based Busbar differential protection. *IEEE Trans Power Deliv*. 2018;33(3):1194-1204. https://doi.org/10.1109/TPWRD.2017.2764058
16. Vasquez FAM, Silva KM. Instantaneous-power-based Busbar numerical differential protection. *IEEE Trans Power Deliv*. 2019;34(2):616-626. https://doi.org/10.1109/TPWRD.2019.2896035
17. Samal L, Samal D, Sahu B. Recognition and classification of multiple power quality disturbances with S-transform and fast S-transform using ELM based classifier. Paper presented at: Proceedings of the 2nd International Conference on Data Science and Business Analytics, ICDSBA 2018, Changsha, China; December 2018:180-185. https://doi.org/10.1109/ICDSBA.2018.00039.
18. Mishra M, Rout PK, Sahu R, Ray D, Swarup S. Study the performance of S-transform based extreme learning machine for islanding detection in distributed generation; 2017. https://doi.org/10.1109/NPSC.2016.7858851.
19. Hadaeghi A, Samet H, Ghanbari T. Multi extreme learning machine approach for fault location in multi-terminal high-voltage direct current systems. *Comput Electr Eng*. 2019;78:313-327. https://doi.org/10.1016/j.compeleceng.2019.07.022
20. Mishra M, Panigrahi RR, Rout PK. A combined mathematical morphology and extreme learning machine techniques based approach to micro-grid protection. *Ain Shams Eng J*. 2019;10(2):307-318. https://doi.org/10.1016/j.asej.2019.03.011
21. AsghariGovar S, Pourghasem P, Seyedi H. High impedance fault protection scheme for smart grids based on WPT and ELM considering evolving and cross-country faults. *Int J Electr Power Energy Syst*. 2019;107:412-421. https://doi.org/10.1016/j.ijepes.2018.12.019
22. IEEE C37.234–2009 - IEEE guide for protective relay applications to power system buses - IEEE standard; 2009; IEEE. https://ieeexplore.ieee.org/document/5325912/citations#citations. .
23. Manual; SIPROTEC &SS60 centralized numerical busbar protection, Edition NO. 7.
24. Stockwell RG, Mansinha L, Lowe RP. Localization of the complex spectrum: the S transform. *IEEE Trans Signal Process*. 1996;44(4):998-1001. https://doi.org/10.1109/78.492555
25. Pinnegar CR, Mansinha L. The S-transform with windows of arbitrary and varying shape. *Geophysics*. 2003;68(1):381-385. https://doi.org/10.1190/1.1543223
26. Bin Huang G, Zhu QY, Siew CK. Extreme learning machine: theory and applications. *Neurocomputing*. 2006;70(1–3):489-501. https://doi.org/10.1016/j.neucom.2005.12.126
27. Bin Huang G, Zhou H, Ding X, Zhang R. Extreme learning machine for regression and multiclass classification. *IEEE Trans Syst Man Cybern B Cybern*. 2012;42(2):513-529. https://doi.org/10.1109/TSMCB.2011.2168604

How to cite this article: Rahimnejad A, Gil M, Abdoos A, Gadsden SA. A hybrid intelligent busbar protection strategy using hyperbolic S-transforms and extreme learning machines. *Engineering Reports*. 2021;3(12):e12438. https://doi.org/10.1002/eng2.12438

APPENDIX A

The CT parameters and Core specification according to Jiles–Atheton model used for the simulation implemented in PSCAD software are as follows

TABLE A1 Core specification according to Jiles–Atheton model

Domain flexing parameter	c	0.1537
Domain pinning parameter	k	2.55×10^{-7}
Parameter to adjust K with M	β	0.97
Inter-domain coupling	α	3.93×10^{-6}
Saturation anhysteretic magnetization	Ms	1.889×10^{6}
Coefficient 1 of anhysteretic curve	α1	2896
Coefficient 2 of anhysteretic curve	α2	3054
Coefficient 3 of anhysteretic curve	α3	17,245
Coefficient 4 of anhysteretic curve	b	2

TABLE A2 Simulated CTs parameters

Turn ratio	2000:5
Secondary resistance	0.35
Area, m^2	17×10^{-4}
Path length, m	0.95
Frequency, Hz	50
Rated voltage, kV	400